

JOURNALS ▼

TOPICS ▼

BOOKS

OTHER PUBLICATIONS ▼



Membership

AGU.org

Advertisement

Find or serve as a mentor to
the global Earth and space sc
mentoring365.chronus.com MENTOR

Geophysical Research Letters*

Space Sciences | [Free Access](#)

A synoptic view of solar transient evolution in the inner heliosphere using the Heliospheric Imagers on STEREO

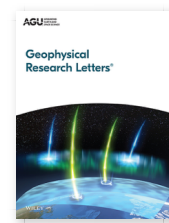
J. A. Davies , R. A. Harrison, A. P. Rouillard, N. R. Sheeley Jr., C. H. Perry, D. Bewsher, C. J. Davis, C. J. Eyles, S. R. Crothers, D. S. Brown

First published: 23 January 2009 |

<https://doi.org/10.1029/2008GL036182> | Citations: 153

Abstract

[1] By exploiting data from the STEREO/heliospheric imagers (HI) we extend a well-established technique developed for coronal analysis by producing time-elongation plots that reveal the nature of solar transient activity over a far more extensive region of the heliosphere than previously possible from coronagraph images. Despite the simplicity of these plots, their power in demonstrating how the plethora of ascending coronal features observed near the Sun evolve as they move



Volume **36**,
Issue **2**

January 2009



Figures References Related Inform.

Recommended

[The Outer Heliosphere](#)

W.I. Axford, S.T. Suess

From the Sun: Auroras,
Magnetic Storms, Solar
Flares, Cosmic Rays, [1]

[Hydrogen atom lifetimes in the three-dimensional heliosphere over the solar cycle](#)

Wayne R. Pryor,
Joseph M. Ajello,
David J. McComas,
Manfred Witte,

antisunward is obvious. The time-elongation profile of a transient tracked by HI can, moreover, be used to establish its angle out of the plane-of-the-sky; an illustration of such analysis reveals coronal mass ejection material that can be clearly observed propagating out to distances beyond 1AU. This work confirms the value of the time-elongation format in identifying/characterising transient activity in the inner heliosphere, whilst also validating the ability of HI to continuously monitor solar ejecta out to and beyond 1AU.

1. Introduction

[2] A valuable technique for characterising Coronal Mass Ejections (CMEs), in terms of such parameters as their ascent profiles and timings, was developed by [Sheeley et al. \[1999\]](#) for application to observations from the LASCO coronagraphs on SOHO [[Brueckner et al., 1995](#)]. This technique involves the creation of a time-height map, constructed by stacking a time series of radial profiles extracted from a sequence of coronagraph images. In such a format, outward-propagating solar transients are manifest as inclined tracks, whose shapes depend on the propagation properties of the individual transients themselves.

[3] Observations from the HI instruments on the pair of NASA STEREO spacecraft can be used to extend the outer limit of this type of presentational format far beyond the 8° elongation limit of the outermost C3 LASCO coronagraph (elongation is the angle between the line to Sun-centre and the line-of-sight). Indeed using HI alone we can instantly reveal the nature of solar transient activity over a region of the heliosphere extending out from around 4 to 90° elongation; this provides a unique method for investigating transient evolution in the inner heliosphere. As STEREO

W. Kent Tobiska

**Journal of Geophysical
Research: Space Physics**

[Transient Phenomena
in the Solar
Atmosphere and Solar
Wind](#)

J.T. Gosling

Physics of Solar Planetary
Environments:
Proceedings of the
International Symposium
on Solar—Terrestrial
Physics, June 7–18, 1976
Boulder, Colorado,
Volume I, [1]

[Statistical study of
magnetic cloud erosion
by magnetic](#)

provides vantage points away from the Sun-Earth line, time-elongation plots produced using HI are especially valuable as they include events, such as CMEs, directed toward Earth.

[4] For HI it is more appropriate to use elongation than height, as knowledge of transient geometry is necessary to convert elongations to distances. In fact, a particularly useful aspect of the time-elongation analysis of HI observations is that the time-elongation profile extracted for a given solar transient can be fitted to provide an estimate of its direction of propagation, as well as its velocity [[Rouillard et al., 2008](#); [Sheeley et al., 2008a, 2008b](#)]. Knowledge particularly of the latter enables a better estimate of the true height profile of a transient to be derived, without the need for plane-of-the-sky approximations frequently used in coronagraph analysis. This is a significant advance, not only for studies of Earth-impacting solar ejecta but also for studying the global nature of transient activity as a function of distance from the Sun. Although touched upon by [Rouillard et al. \[2008\]](#) and [Sheeley et al. \[2008a, 2008b\]](#), here we detail the methodology used to optimise the time-elongation format to best exploit STEREO/HI observations, and illustrate its usage based on observations from an interval in July 2007 characterised by significant CME activity.

2. Instrumentation

[5] The STEREO spacecraft were launched in October 2006 into heliocentric orbits of approximately 1AU radius. STEREO-A leads the Earth in its orbit, while STEREO-B trails the Earth; the angular separation between each spacecraft and the Earth increases by approximately 22.5° every year. In addition to a complement of in-situ instrumentation, each STEREO spacecraft carries the SECCHI imaging suite [[Howard et al., 2008](#)] which comprises an Extreme Ultraviolet Imager (EUVI), two Sun-centred coronagraphs

ultraviolet imager (EUVI), two sun centered coronagraphs (COR1 and COR2), and HI. The HI instrument [[Eyles et al., 2009](#)] consists of two visible-light cameras, HI-1 and HI-2. The HI-1 camera has a $20 \times 20^\circ$ field-of-view (fov) with its boresight directed at 14° elongation; the boresight of the 70° wide HI-2 fov is aligned at 53.7° . The HI boresights are nominally aligned in the ecliptic plane; however, this was not the case in particular during the initial phase of the mission. STEREO/HI builds upon the heritage of space-based wide-field heliospheric imaging of the Solar Mass Ejection Imager (SMEI) on the Coriolis spacecraft [[Eyles et al., 2003](#)]. Here we present observations from the HI cameras on STEREO-A, designated HI-1A and HI-2A.

3. Observations

[6] As with conventional coronagraphs, the HI cameras detect photospheric light scattered from free electrons in the K-corona and from interplanetary dust around the Sun (the F-corona), as well as light from the stars together with any planets and other visual objects within the fov. The intensity of the F-corona and many brighter stars far exceeds that typical of K-coronal transients [[Eyles et al., 2009](#)]. A method applied extensively to coronagraph images to facilitate investigation of the motion of faint K-coronal features is the running difference technique [[Sheeley et al., 1997](#)], in which each image is presented with the previous image subtracted. Hence what is viewed is the change in intensity over the fov between the current and previous image. Image differencing substantially reduces the F-coronal contribution to the HI images, the F-corona being stable on timescales far longer than the nominal image cadence of 40 and 120 minutes for the HI-1 and HI-2 cameras, respectively, such that much of what remains is K-corona. As the K-corona is illuminated via Thomson scattering, image differencing highlights changes in electron density between adjacent images, revealing regions of

density enhancement and depletion.

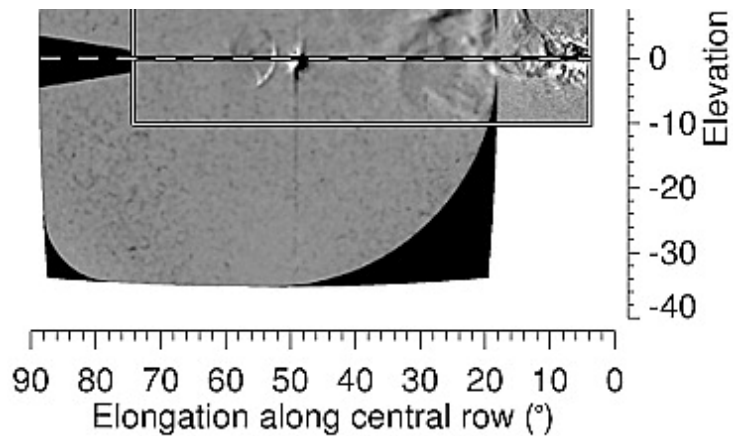
[7] The progression of each STEREO spacecraft around its orbit leads to a drift of the star field through the HI fovs by some 2.5 arcmin/hr. This corresponds to a motion of approximately 1 pixel between adjacent images for both HI-1 and HI-2, the higher cadence of the HI-1 images being offset by its smaller pixel size compared to HI-2 (note that the synoptic science images for both cameras comprise 1024×1024 binned pixels - the word pixel is used to refer to a binned pixel throughout). The stellar contribution to the difference images can be appreciably reduced by aligning each image pair in Geocentric Equatorial Inertial (GEI) coordinates prior to differencing. Since the STEREO spacecraft follow Earth-like orbits around the Sun, at distances small compared to the distances to other stars, GEI adequately represents the positions of stars viewed therefrom. Image alignment requires precise determination of HI instrument attitude. We therefore take advantage of the work of [Brown et al. \[2009\]](#) who use star positions in an image to provide a more accurate determination of the HI pointing direction than was previously available, as well as deriving updated values for the optical characteristics of the cameras.

[8] Due to the presence of large spatial gradients in the F-corona, introducing a shift between adjacent images to align in GEI necessitates the prior subtraction of an F-coronal background from each image. As an estimate of the background for an image we use the minimum intensity observed in each pixel for all images taken by that camera within a 7-day interval centred on the day that the image was taken. Note that the above processing is supplemental to the standard HI calibration procedures, such as shutterless correction and flat-fielding [[Eyles et al., 2009](#)].

Figure 1a illustrates the relative positions and angular

[2] [Figure 1a](#) illustrates the relative positions and angular extents of the HI-1 and HI-2 fovs by combining running difference images from the two cameras onboard STEREO-A from 18UT on 12 July 2007; observations from the outer HI-2A camera are plotted where the two fovs overlap. The axes are given in terms of elongation along the centre line of the combined image (dashed line) and elevation angle perpendicular to that line; note that all values of elongation subsequently referred to in the text are along the centre line. Throughout the entire interval presented in this paper, the roll of STEREO-A from ecliptic north around its principal Sun-aligned axis was less than 1° . Consequently, since the orbital planes of the STEREO spacecraft are closely aligned with the ecliptic plane, the latter corresponds to a line that runs approximately along the centre of the combined HI image. This is confirmed by the position on the centre line, near 50° elongation, of the signature of Venus; some vertical bleeding of the saturated image along CCD detector columns is also visible. The semi-circular feature beyond Venus results from ghosting of its image in the camera optics. Camera distortion due to imaging properties of the wide-angle optics has been accounted for in the angular projection; this is particularly pronounced for HI-2 [[Eyles et al., 2009](#)]. A mask is applied to the HI-2A image to conceal areas of the fov obscured by both the stray-light baffle system and the Earth occulter that obscures the outer edge of the central portion of the HI-2 fov. The difference in their respective cadences means that, although combined as a single (albeit difference) image, the HI-1A and HI-2A images in each panel are not strictly simultaneous.





b) 06 UT, 12 July 2007

c) 12 UT, 12 July 2007

d) 18 UT, 12 July 2007

e) 06 UT, 13 July 2007

f) 18 UT, 13 July 2007

g) 06 UT, 14 July 2007

h) 06 UT, 15 July 2007

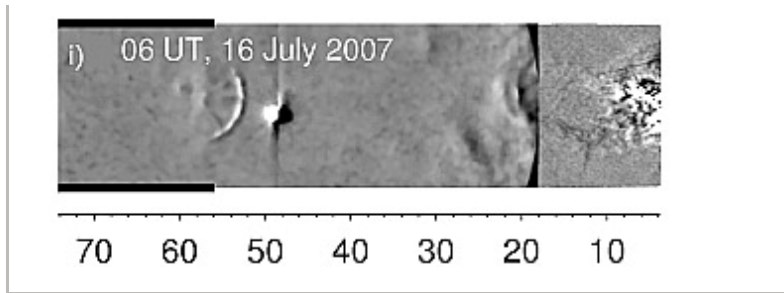


Figure 1 [Open in figure viewer](#) | [PowerPoint](#)

(a) Running difference images from HI-1A and HI-2A illustrating the geometrical arrangement of their fovs. (b–i) Series of such images showing the passage of a CME through the HI-1A and HI-2A fovs.

[10] In addition to the processing discussed above, a degree of smoothing is applied to reduce the residual stellar signal and other noise in the difference images. To this end, each pixel is replaced by the robust mean of its 7×7 pixel neighbourhood, where values outside two standard deviations are disregarded in determining the final mean.

[11] [Figures 1b–1i](#) illustrate a sequence of such combined HI-1A/HI-2A running difference images, covering the interval 06UT on 12 July to 06UT on 16 July 2007 (although not equally separated in time). Here we are primarily interested in the passage of solar transients in the ecliptic. Thus in [Figures 1b–1i](#) we only display that portion of the combined HI image bounded by the rectangle marked on [Figure 1a](#), which is centred on the centre line of the combined image which lies approximately in the ecliptic plane. Coverage in elevation angle encompasses the full extent of the HI-1A fov in that dimension, approximately 20° . Elongation extends from 4° at the inner edge of the inner HI-1A fov to around 74° , a limit imposed by the positioning of the Earth occulter in the HI-2A fov. [Figure 1d](#) corresponds to a truncated version of [Figure 1a](#). In these images, an outward-propagating region of enhanced electron density is manifest

as a positive (light grey/white) followed by a negative (dark grey/black) intensity perturbation, corresponding to regions of enhanced and reduced density, respectively.

[12] [Figures 1b–1i](#) reveal much coronal activity. However, of principal interest to us is the CME that is confined to elongations of less than 13° (i.e. within the HI-1A fov) at 06UT on 12 July ([Figure 1b](#)); the approximate elongation extent of this CME is indicated on each panel using horizontal bars. Features observed simultaneously at larger elongations are associated with an earlier CME, the most intense signatures of which propagate north of the ecliptic. Despite its complexity, the CME of interest can be traced quite clearly through the combined fov, entering the HI-2A fov by 18UT on 12 July ([Figure 1d](#)). Although preceded by a hierarchy of overlying loops, the most conspicuous signature of this CME is a V-shaped structure that can be first distinguished from the background coronal variations around 12UT on 12 July having expanded out to 16° elongation ([Figure 1c](#)). This feature propagates through the HI-1A fov before entering the HI-2A fov between 06 ([Figure 1e](#)) and 18UT ([Figure 1f](#)) the following day. By 06UT on 16 July, this feature, although faint, can still be discriminated having propagated out to almost 60° elongation ([Figure 1i](#)).

[13] Although our primary objective is reporting the more generic development of display and analysis methods for the study of heliospheric transients observed by STEREO/HI, we note that this CME is suggested by simple back-projection to have been launched early on 11 July, from an area on the eastern (relative to the Sun-Earth line) solar limb associated with NOAA active region 10963. It subsequently propagated through the fovs of the inner (COR1) and outer (COR2) coronagraphs on STEREO-A and -B, and both the inner (C2) and outer (C3) SOHO/LASCO coronagraphs. [Figures 1b](#) and [1i](#) correspond to times approximately 24 and 120 hours after the projected CME launch time. Both

and 120 hours after the projected CME launch time. Both STEREO/EUVI instruments and the analogous EIT instrument on SOHO reveal large-scale coronal disruptions in the vicinity of active region 10963 in the 171 and 195Å wavebands throughout this and the previous day. Activity was confirmed by the geostationary GOES satellite, which detected multiple B- and C-class X-ray flares.

[14] Although initially discernable in the coronagraph images at 04UT on 11 July, as a twisted emerging coronal loop, by 20UT (when well into the COR2 and C3 fovs) the CME had developed a three-part structure, comprising an outer loop followed by a low density cavity in which is embedded a dense core. This commonly observed CME morphology is reflected in the HI images ([Figure 1](#)), with the outer loops and (in this case V-shaped) core, separated by a void. The outward-concave nature of the CME core observed by HI is echoed at lower heights in the coronagraph observations. Previous observations of CME-associated V-shaped coronal structures by LASCO and SMEI have been explained in terms of magnetic reconnection [[Simnett et al., 1997](#)], line-of-sight integration along a horizontal flux rope [[Wang and Sheeley, 2006](#)], and interaction of the CME with the solar wind [[Kahler and Webb, 2007](#)].

[15] The time-elongation plot presented in [Figure 2](#) is produced by stacking the intensities along the centre line of a sequence of combined HI-1A and HI-2A running difference images from July 2007, such as and including those in [Figure 1](#). [Figure 2](#) covers the interval 6 to 26 July, which includes the passage of the aforementioned CME together with a host of other outward-propagating features. Like [Figures 1b–1i](#), [Figure 2](#) extends in elongation from the sunward edge of the HI-1A fov to the edge of the HI-2A occulter, a coverage of 4 to 74° along the centre line which corresponds closely to the ecliptic throughout. As the signal

within a pixel is the line-of-sight integral along a fixed direction, a specific elongation does not correspond to a unique height above the solar surface. However, as discussed later, the true height profile of a solar transient observed by HI can actually be derived from its elongation variation.

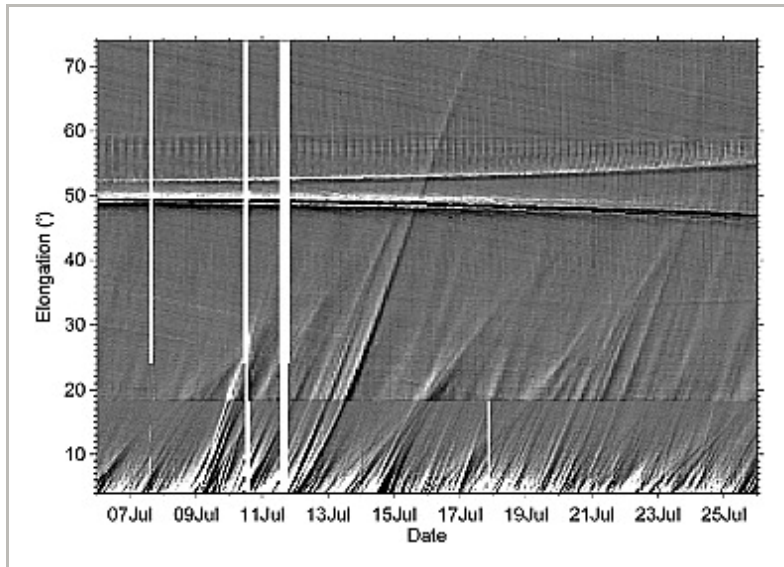


Figure 2 [Open in figure viewer](#) | [PowerPoint](#)

Time-elongation plot constructed from running difference observations along the central rows of the HI-1A and HI-2A fovs.

[16] To enhance the signal from faint coronal transients, what is presented is not simply a stacked time series of the central row extracted from each combined difference image. Instead, for each column the robust mean of the central 64 rows is evaluated. Again, HI-2A observations are plotted where the HI-1A and HI-2A fovs overlap. Before discussing the signatures of solar origin, we mention a number of other features visible in [Figure 2](#). Vertical white bars denote missing images in either/both cameras. The faint background of sunward-moving parallel lines corresponds to the remnant of the star field not entirely removed by the processing. The feature that migrates sunward from 50 to 47° elongation through the interval

sunward from 50 to 47° elongation through the interval corresponds to the image of Venus in the HI-2A fov; the feature moving antisunward, from 52 to 55°, corresponds to Venus' ghost image.

[17] The time-elongation format provides an excellent means of revealing the evolution of solar ejecta over extended time intervals, in this case in the ecliptic plane. Presenting the STEREO/HI observations in this way enables us to instantly visualise outward-moving solar transients over a region that extends out to over ten times the maximum elongation covered by LASCO and, indeed, twenty times further out than the images from the coronagraphs onboard STEREO. Clearly we are extending a coronal monitoring technique to the analysis of heliospheric phenomena. These observations were made by STEREO-A from a vantage point 11° off the Sun-Earth line. Use of this unique perspective will be further enhanced as the mission progresses, when increased inter-spacecraft separation will afford us the most effective use of simultaneous observations from the two STEREO spacecraft.

[18] As noted above, [Figure 2](#) reveals an abundance of inclined tracks, indicating antisunward-moving solar transients. The variety of forms exhibited by these signatures, over a relatively limited time interval, suggests a great diversity of propagation characteristics manifested by solar ejecta. Many appear not to trace out a simple linear trajectory but exhibit gradual changes in their slope. Although such changes may indicate a real acceleration or deceleration of solar transients, at the elongations monitored by HI it is more likely to be a result, and an extremely useful one, of observing geometry.

[19] A striking feature of the time-elongation plot is the distinct reduction in the number of antisunward-propagating solar transients observed at increasing

elongations; note this does not refer to the discontinuity near 18° caused by the different HI-1/HI-2 instrument sensitivities. Below around 10° , large numbers of outward-moving features are apparent; it is the highly dynamic region below 8° elongation that is viewed by LASCO and the STEREO/COR coronagraphs. Beyond these elongations, many such features appear to fade out. This is likely due to a combination of a number of factors, including the reduction in their intensities below the observational sensitivity as they expand radially outward and merge into the background solar wind structure. Another contributory factor would be the reduction in scattering efficiency if the transients diverge from the Thomson scatter sphere, the surface of maximum scattering [[Vourlidas and Howard, 2006](#)], as they propagate outward. Nevertheless, about 20 events are still visible out to 30° elongation, and a small number beyond even that. This simplification of the solar wind structure away from the Sun is surely a fundamental feature of the inner heliosphere. The time-elongation plot graphically illustrates major differences between the active inner heliosphere, within the first ten or so degrees, and the much more large-scale structuring of the solar wind at Earth-like distances.

[20] One transient is conspicuous in that it can be clearly tracked across the entire elongation range of [Figure 2](#). This feature, which enters the HI-1A fov near 00UT on 12 July and propagates antisunward until it finally becomes obscured by the HI-2A occulter late on 17 July, corresponds to the CME imaged in [Figure 1](#) and launched from the eastern solar limb on 11 July. It is the ascending dense CME core material that produces this, the clearest signal. Note the transition between light and dark within the core trace results from use of difference images. Leading the CME core, yet separated from it by the cavity region, are the fainter tracks of the complex hierarchy of outer loops.

[21] [Sheeley et al. \[2008a, 2008b\]](#) and [Rouillard et al. \[2008\]](#) have demonstrated that in viewing a solar transient propagating at a constant speed out to large elongations, HI will not record a simple linear trajectory. Instead, the trajectory will exhibit a particular shape depending upon the longitude of propagation of the transient relative to the Sun-spacecraft line and its radial speed. Analysis of the elongation variation of the CME core material returns a best fit for a longitude 48° east of the Sun-STEREO-A line and a radial speed of 320 km s^{-1} ; in principle such analysis can be applied to the ascending profile of any signature in a plot such as [Figure 2](#). We note that this fitted value for its longitude of propagation, bearing in mind the location of STEREO-A at the time (11° ahead of Earth), is consistent with the CME being associated with active region 10963. This region was located 38° east of the central meridian as seen from SOHO at 04UT on 11 July, the time when the CME was first discernable in coronagraph observations. The fitted parameters provide an estimate for the CME launch time of 13UT on 11 July. This does not account for the possibility of true acceleration near the Sun, so is not incompatible with a launch time nearer 04UT. Given the premise of the STEREO mission and in particular HI instrument concept, more interesting than the launch time of the CME is the distance over which it can be observed. The CME can be clearly tracked in the ecliptic until it becomes obscured by the occulter at 74° elongation. For its longitude of propagation, this corresponds to a distance from the Sun of 1.1AU. It is worth pointing out that for such a low velocity CME, it is unlikely that the concave nature of the CME core is due to a wind shear effect. Only by using multi-spacecraft, in-situ observations could one distinguish between the two alternative explanations of magnetic reconnection and line-of-sight integration effects.

[22] We have focused on a generalised description of the

... the more general description of the application of the time-elongation technique to HI observations. Although illustrated through reference to a particular CME, other phenomena can certainly be identified from such displays, for example Corotating Interaction Regions (CIRs) [[Rouillard et al., 2008](#); [Sheeley et al., 2008a, 2008b](#)]. In fact, the family of converging tracks observed most clearly by HI-2A between 19 and 22 July constitutes a typical CIR signature as observed by HI on STEREO-A [[Sheeley et al., 2008a](#); [Rouillard et al., 2008](#)].

4. Conclusions

[23] The STEREO/HI instruments herald a major advance in the study of the propagation and evolution of solar transients in the inner heliosphere, in particular those directed towards Earth. They enable, for the first time, solar transients to be imaged continuously out to 90° elongation from vantage points away from the Sun-Earth line. The principal aim of this paper is to demonstrate the power of presenting the HI observations in a time-elongation format based on that developed to display coronagraph observations. In doing so, the scope of this type of plot is expanded beyond its original goal of characterising the temporal behaviour of the near-solar corona to illustrating the nature and behaviour of solar ejecta over much of the inner heliosphere, out to and beyond 1AU. The time-elongation map of combined HI-1 and HI-2 observations from the STEREO-A spacecraft for an interval in July 2007 reveals a plethora of ascending solar transients. Whilst many such features appear to dissipate or merge close to the Sun, a significant fraction persist out to several tens of degrees elongation. This technique powerfully illustrates the fundamental evolution of the heliosphere outward from the Sun.

[24] One antisunward-propagating solar transient, a CME,

can be clearly tracked across the entire elongation range covered by HI along the ecliptic, 4 out to 74°. A fit to the time-elongation profile of its dense core provides estimates of its longitude and velocity consistent with the CME launch having been associated with an active region within the streamer belt on the eastern solar limb. In-situ observations from the Venus Express spacecraft indicate that it passed through the piled-up sheath region surrounding this CME; Venus' location relative to the predicted longitude of propagation of the CME suggests a CME half-width of less than 12°. Observations from the Messenger spacecraft, predicted to be in the direct path of this CME, are under analysis. This is one of the first CMEs to be observed clearly to the limit of the HI fov, which for its longitude corresponds to a distance 1.1AU from the Sun, thereby validating the efficacy of STEREO/HI in the study of the propagation of solar transients to and beyond Earth-like distances.

Acknowledgments

[25] STEREO/HI was developed by a consortium comprising RAL, the University of Birmingham (UK), CSL (Belgium) and NRL (USA). SECCHI, led by NRL, involves additional collaborators from LMSAL, GSFC (USA), MPI (Germany), IOTA and IAS (France).

References



Brown, D. S., D. Bewsher, and C. J. Eyles (2009), Calibrating the pointing and optical parameters of the STEREO heliospheric imagers, *Sol. Phys.*, **254**, 185.

[Crossref](#) | [ADS](#) | [Web of Science®](#) | [Google Scholar](#)

Brueckner, G. E., et al. (1995), The Large Angle Spectroscopic Coronagraph (LASCO), *Sol. Phys.*, **162**, 357.

[Crossref](#) | [ADS](#) | [Web of Science®](#) | [Google Scholar](#)

Eyles, C. J., et al. (2003), The Solar Mass Ejection Imager (SMEI), *Sol. Phys.*, **217**, 319.

[Crossref](#) | [ADS](#) | [Web of Science®](#) | [Google Scholar](#)

Eyles, C. J., et al. (2009), The heliospheric imagers on-board the STEREO mission, *Sol. Phys.*, in press.

[Crossref](#) | [ADS](#) | [Web of Science®](#) | [Google Scholar](#)

Howard, R. A., et al. (2008), Sun Earth Connection Coronal and Heliospheric Investigations (SECCHI), *Space Sci. Rev.*, **136**, 67.

[Crossref](#) | [CAS](#) | [ADS](#) | [Web of Science®](#) | [Google Scholar](#)

Kahler, S. W., and D. F. Webb (2007), V arc interplanetary coronal mass ejections observed with the Solar Mass Ejection Imager, *J. Geophys. Res.*, **112**, A09103, doi:10.1029/2007JA012358 .

[Wiley Online Library](#) | [ADS](#) | [Web of Science®](#) | [Google Scholar](#)

Rouillard, A. P., et al. (2008), First imaging of corotating interaction regions using the STEREO spacecraft, *Geophys. Res. Lett.*, **35**, L10110, doi:10.1029/2008GL033767 .

[Wiley Online Library](#) | [ADS](#) | [PubMed](#) | [Web of Science®](#) | [Google Scholar](#)

Simnett, G. M., et al. (1997), LASCO observations of disconnected magnetic structures out to and beyond 28 solar radii during coronal mass ejections, *Sol. Phys.*, **175**, 685.

[Crossref](#) | [ADS](#) | [Web of Science®](#) | [Google Scholar](#)

Sheeley, N. R., et al. (1997), Measurements of flow speeds in the corona between 2 and 30 solar radii, *Astrophys. J.*, **484**, 472.

[Crossref](#) | [ADS](#) | [Web of Science®](#) | [Google Scholar](#)

Sheeley, N. R., J. H. Walters, Y.-M. Wang, and R. A. Howard (1999), Continuous tracking of coronal outflows: Two kinds of coronal mass ejection, *J. Geophys. Res.*, **104**, 24,739.

[Wiley Online Library](#) | [ADS](#) | [Web of Science®](#) | [Google Scholar](#)

Sheeley, N. R., et al. (2008a), SECCHI observations of the Sun's garden-hose density spiral, *Astrophys. J.*, **674**, 109.

[Crossref](#) | [ADS](#) | [Web of Science®](#) | [Google Scholar](#)

Sheeley, N. R., et al. (2008b), Heliospheric images of the solar wind at Earth, *Astrophys. J.*, **675**, 853.

[Crossref](#) | [ADS](#) | [Web of Science®](#) | [Google Scholar](#)

Vourlidas, A., and R. A. Howard (2006), The proper treatment of coronal mass ejection brightness: A new methodology and implications and observations, *Astrophys. J.*, **642**, 1216.

[Crossref](#) | [ADS](#) | [Web of Science®](#) | [Google Scholar](#)

Wang, Y.-M., and N. R. Sheeley Jr. (2006), Observations of flux rope formation in the outer corona, *Astrophys. J.*, **650**, 1172.

[Crossref](#) | [ADS](#) | [Web of Science®](#) | [Google Scholar](#)

Citing Literature



[Download PDF](#)

[Back to Top](#)



[AGU PUBLICATIONS](#)

[AGU.ORG](#)

[AGU MEMBERSHIP](#)

[Author Resources](#)

[Contact AGU](#)

[Editor Searches](#)

[Librarian Resources](#)

[Media Kits](#)

[Publication Award](#)

[Publication Policies](#)

[Scientific Ethics](#)

[Submit a paper](#)

[Usage Permissions](#)



© 2022 American
Geophysical Union

About Wiley
Online Library

Privacy Policy

Terms of Use

Cookies

Accessibility

Publishing Policies

Help & Support

Contact Us

Training and
Support

DMCA & Reporting
Piracy

Opportunities

Subscription
Agents

Advertisers &
Corporate Partners

Connect with
Wiley

The Wiley Network

Wiley Press Room

Copyright © 1999-2022 John Wiley & Sons, Inc. All rights reserved

WILEY